



Fermi National Accelerator Laboratory

FERMILAB-Pub-86/107-TA

July, 1986

Resonant Solar Neutrino Oscillation Experiments

Stephen J. Parke and Terry P. Walker

Fermi National Accelerator Laboratory

P.O. Box 500, Batavia, Illinois, 60510

Abstract

The results of a detailed calculation of the effects of resonant neutrino oscillations in the sun on the current and proposed solar neutrino experiments are presented. Analytic results are used for the electron neutrino survival probability so that a sophisticated model for both the production distribution of the solar neutrino sources and the solar electron number density can be employed. Contour plots for the electron neutrino capture rate, in the mass difference squared versus vacuum mixing angle plane, are given for the current ^{37}Cl experiment and the proposed ^{71}Ga detector.



Resonant Solar Neutrino Oscillation Experiments

Stephen J. Parke and Terry P. Walker

Fermi National Accelerator Laboratory

P.O. Box 500, Batavia, Illinois, 60510

Abstract

The results of a detailed calculation of the effects of resonant neutrino oscillations in the sun on the current and proposed solar neutrino experiments are presented. Analytic results are used for the electron neutrino survival probability so that a sophisticated model for both the production distribution of the solar neutrino sources and the solar electron number density can be employed. Contour plots for the electron neutrino capture rate, in the mass difference squared versus vacuum mixing angle plane, are given for the current ^{37}Cl experiment and the proposed ^{71}Ga detector.

Recently, Mikheyev and Smirnov¹ have shown that the matter neutrino oscillations of Wolfenstein² can undergo resonant amplification in the solar interior thereby reducing the flux of electron neutrinos emerging from the Sun. This mechanism may be the solution to the solar neutrino puzzle^{3,4}. Subsequently, Bethe and others^{5,6} have refined and restated the Mikheyev and Smirnov idea, pointing out that there are three general regions of parameter space in which the solar electron neutrino flux is sufficiently reduced. Unfortunately, all of these papers either use a crude solar model or do not consider the non-adiabatic region of parameter space.

In this letter, we correct this deficiency and present contour plots of electron neutrino capture rates in the mass difference squared - vacuum mixing angle plane, for both chlorine experiment and the proposed gallium detector. These plots are the results of detailed calculations of the solar electron neutrino capture rates in ³⁷Cl and ⁷¹Ga as a function of mass difference squared and vacuum mixing angle. We use an analytic form for the neutrino transformation probability which is valid in both the adiabatic and non-adiabatic regime⁷, in conjunction with a relatively sophisticated solar model.

If neutrinos are massive then the flavor and mass eigenstates are not necessarily identical, however a general neutrino state can always be written in the flavor basis⁸,

$$|\nu(t)\rangle = c_e(t) |\nu_e\rangle + c_\mu(t) |\nu_\mu\rangle. \quad (1)$$

In the ultra-relativistic limit, the evolution of this general neutrino state, in matter, is described by the following Schrodinger-like equation²,

$$i \frac{d}{dt} \begin{pmatrix} c_e \\ c_\mu \end{pmatrix} = \frac{1}{2} \begin{pmatrix} -\Delta_0 \cos 2\theta_0 + \sqrt{2}G_F N_e & \Delta_0 \sin 2\theta_0 \\ \Delta_0 \sin 2\theta_0 & \Delta_0 \cos 2\theta_0 - \sqrt{2}G_F N_e \end{pmatrix} \begin{pmatrix} c_e \\ c_\mu \end{pmatrix}, \quad (2)$$

where $\Delta_0 \equiv \delta m^2/2k = (m_2^2 - m_1^2)/2k$, m_i are the neutrino masses, k is the neutrino energy, θ_0 is the vacuum mixing angle, G_F is the Fermi constant and N_e is the electron number density. The matter mass eigenstates, in an electron density N_e , are

$$\begin{aligned}
|\nu_1\rangle &= \cos\theta_N |\nu_e\rangle - \sin\theta_N |\nu_\mu\rangle, \\
|\nu_2\rangle &= \sin\theta_N |\nu_e\rangle + \cos\theta_N |\nu_\mu\rangle
\end{aligned}
\tag{3}$$

where the matter mixing angle, θ_N , is given by $\sin 2\theta_N = \Delta_0 \sin 2\theta_0 / \Delta_N$ with $\Delta_N = [(\Delta_0 \cos 2\theta_0 - \sqrt{2}G_F N_e)^2 + \Delta_0^2 \sin^2 2\theta_0]^{1/2}$. At resonance, the electron density is $N_e^{res} = \Delta_0 \cos 2\theta_0 / \sqrt{2}G_F$, and the matter mixing angle $\theta_N^{res} = \pi/4$. Above resonance, θ_N satisfies $\pi/4 < \theta_N < \pi/2$.

We use the approximation that the electron density in the Sun varies linearly in the region where transitions between the matter mass eigenstates are important. Then the probability of detecting an electron neutrino, averaged over the production and the detection positions, is given by⁷

$$\overline{P_{\nu_e}} = \frac{1}{2} + \left(\frac{1}{2} - P_z\right) \cos 2\theta_0 \cos 2\theta_N
\tag{4}$$

where P_z is the Landau-Zener probability for transitions between the matter mass eigenstates during single resonance crossing:

$$P_z = \exp \left[-\frac{\pi \sin^2 2\theta_0}{2 \cos 2\theta_0} \frac{\delta m^2 / 2k}{|\vec{n} \cdot \nabla \ln N_e|_{res}} \right].
\tag{5}$$

The unit vector, \vec{n} , is in the direction of propagation of the neutrino. For non-resonance crossing $P_z = 0$ and for double resonance crossing, P_z in eqn(4) should be replaced by $2P_z(1-P_z)$. From eqn(4) and (5), one can see that the electron neutrino detection probability depends only on the electron density in the solar interior at production and the logarithmic slope of this density at resonance crossing. In figure 1(a) we give the fit for $N_e(r) = \rho(r)Y_e(r)/m_N$ used in our calculations which was obtained from Bahcall's solar model⁹.

The solar electron neutrino capture rate for a detector characterized by a electron

neutrino capture cross section, $\sigma(E)$, and energy threshold E_0 , is

$$\sum_{\text{processes}} \int_{E_0}^{\infty} \frac{d\Phi_{\nu}}{dE} \sigma(E) dE. \quad (6)$$

The sum is taken over all neutrino sources in the Sun and $d\Phi_{\nu}/dE$ is the differential electron neutrino flux of a given source at the earth's surface. To include the reduction in the electron neutrino flux from the Sun due to resonant neutrino oscillations, the differential electron neutrino flux for each process was calculated as

$$\frac{d\Phi_{\nu}}{dE} \propto W(E) \int_{\text{sun}} dV \overline{P_{\nu_e}} \frac{df}{dV} \quad (7)$$

where $W(E)$ is the standard weak interaction energy distribution for the neutrinos of a given process and df/dV is the fraction of the standard solar model flux coming from a given solar volume element for this process. In figure 1(b) we have plotted $r^2 df/dV$ for the various processes, which were calculated from Bahcall's solar model. Note, we have assumed that the spatial distributions for pep and CNO neutrinos are given by those for pp and ${}^8\text{B}$ neutrinos, respectively¹⁰. We normalize $d\Phi_{\nu}/dE$ for each process by demanding that the energy and solar volume integrations of eqn.(6) yield the capture rates quoted by Bahcall when $\overline{P_{\nu_e}} = 1$.

The cross sections, $\sigma(E)$, used for the ${}^{37}\text{Cl}$ and ${}^{71}\text{Ga}$ detectors, whose thresholds are 814 and 236 keV respectively, are given in figure 2. The ${}^{37}\text{Cl}$ cross section is derived from the data of Bahcall⁹ and the ${}^{71}\text{Ga}$ cross section is a fit to the low energy calculation of Bahcall¹¹ and the higher energy calculations of Grotz, Klapdor, and Metzger¹². In Table I, we list two sets of expected capture rates for both the chlorine and gallium experiments and the maximum neutrino energy for each solar neutrino source. Model A is taken from the values of Bahcall *et al.*⁴ and Model B, reported by Bahcall¹³, reflects recent changes in the expected solar neutrino capture rate. The most important change being in the estimation of the Sun's opacity which alters the solar temperature profile. A comparison between these two models demonstrates the insensitivity of the allowed

region of parameter space to small changes in the solar model. The value of 16 SNU for the ${}^8\text{B}$ rate in Model A for the gallium experiment is an average of the new predictions of Grotz *et al.* and Mathews *et al.*¹⁴.

In figures 3 and 4, we present electron neutrino capture rate contours (iso-SNU contours) for the ${}^{37}\text{Cl}$ and ${}^{71}\text{Ga}$ experiments as a function of δm^2 and $\sin^2 2\theta_0 / \cos 2\theta_0$ for the two solar models discussed earlier. The 3σ deviations from the Davis *et al.*³ result of 2.1 SNU are the 2.4 and 1.8 iso-SNU contour lines in fig 3. The similarity of the shape of these plots for the two solar models reflects the insensitivity of the resonant oscillation process to small changes in the structure of the Sun. However, the position of individual contours does change, due to changes in the contributions from the individual neutrino sources. The generic structure of these total SNU plots is due to the superposition of triangular iso-SNU contours associated with each individual neutrino source contributing to a given total SNU value. These individual contours owe their shape to the appropriate iso-probability contour⁷ and their position is determined by the typical energy scale and production electron density of the individual neutrino source. For each neutrino source the resonance mechanism becomes important, provided $\theta_0 > 0.01$, as soon as δm^2 becomes small enough so that the average resonant electron density for that source is less than the solar electron density at the production site. This occurs when δm^2 is approximately equal to 1.5×10^{-4} , 1.2×10^{-5} , and 3.7×10^{-6} eV² for the ${}^8\text{B}$, ${}^7\text{Be}$ and pp neutrinos respectively. Below these values the individual neutrino sources have contours which are diagonals of slope minus one coming from the form of the transition probability between adiabatic states, eqn(5). The intersection of these diagonal lines with the turning on of resonance for ${}^8\text{B}$, ${}^7\text{Be}$ and pp is responsible for the shoulders at small $\sin^2 2\theta_0 / \cos 2\theta_0$ in the contour plots. The vertical sections of the contours, at large θ_0 , occurs because for large θ_0 both adiabatic states have a large component of electron neutrino.

From fig(4), we see that the results of the ^{71}Ga experiment can range from 10 to 120 SNU and still be compatible with the ^{37}Cl experiment. In general, a given gallium contour crosses the 2.1 ± 0.3 chlorine contour at least twice and therefore the results of the ^{71}Ga experiment will leave a two-fold degeneracy in $(\delta m^2, \theta_0)$ -space. If one accepts the theoretical prejudice against large vacuum angles provided by see-saw models¹⁵, this degeneracy is removed. Unfortunately, the degeneracy is continuous for that region of parameter space corresponding to a ^{37}Cl rate of 2.1 ± 0.3 SNU and a ^{71}Ga rate greater than 100 SNU. In this region *only* the ^8B neutrinos are effected by the resonance phenomena. Also, in this region of parameter space the two experiments will not be able to distinguish between a small temperature change at the solar core and the resonant neutrino oscillation mechanism. This is due to the relatively strong temperature dependence of the ^8B neutrino flux¹⁶. It is only when the ^{71}Ga SNU rate is depleted below that of merely removing the ^8B component (*i.e.*, appreciably less than 110 SNU), so that reduction of the less temperature sensitive neutrinos (^7Be and pp) becomes necessary, that the resonant oscillation mechanism becomes a likely solution to the solar neutrino problem.

Acknowledgements

We would like to thank Rocky Kolb for making us aware of John Bahcall's new results and John Bahcall for discussing the changes which give rise to his new model.

References

1. S.P. Mikheyev and A.Yu. Smirnov, *10th International Workshop on Weak Interactions and Neutrinos*, Savonlinna, Finland(1985); *Nuovo Cimento* **C9**, 17(1986).
2. L. Wolfenstein, *Phys. Rev.* **D17**, 2369(1978); *Phys. Rev.* **D20**, 2634(1979).
3. R. Davis, D.S. Harmer, and K.C. Hoffman, *Phys. Rev. Letters* **20**, 1205(1968).
4. J.N. Bahcall, B.T. Cleveland, R. Davis, and J.K Rowley, *Astrophys. J.* **292**, L79(1985).
5. H.A. Bethe, *Phys. Rev. Letters* **56**, 1305(1986).
6. A. Messiah and S.P. Rosen and M. Spiro, *1986 Massive Neutrinos in Astrophysics and in Particle Physics*, Tignes, January 1986; S.P. Rosen and J.M. Gelb, Los Alamos National Laboratory Preprint, March 1986; E.W. Kolb, M.S. Turner, and T.P. Walker, Fermilab Preprint-Pub-86/69-A, April 1986; V. Barger, R.J.N. Phillips, and K. Whisnant, University of Wisconsin Preprint, MAD/PH/280, April 1986.
7. S. Parke, Fermilab Preprint, Pub-86/67-T, May 1986.
8. The other flavor eigenstate could just as well be ν_τ .
9. J.N. Bahcall, W.F. Huebner, S.H. Lubow, P.D. Parker, and R.K. Ulrich, *Rev. Mod. Phys.* **54**, 767(1982).
10. The CNO distributions are undoubtedly tighter than ${}^8\text{B}$ due to their more sensitive dependence on temperature, but the inaccuracy introduced by this approximation is negligible.
11. J.N. Bahcall, in *Proceedings of the Neutrino Mass Miniconference*, eds. V. Barger and D. Cline, Telemark, Wisconsin(1980).

12. K. Grotz, H.V. Klapdor, and J. Metzinger, *Astron. Astrophys.* **154**, L1(1986).
13. J. N. Bahcall, *International Symposium on Weak and Electromagnetic Interactions in Nuclei*, Heidelberg, July 1986.
14. G.J. Mathews, S.D. Bloom, G.M. Fuller, and J.N. Bahcall, *Phys. Rev.* , **C32**, 796(1985).
15. T. Yanagida, *Prog. Theor. Phys.* **B135**, 66(1978); M. Gell-Mann, P. Ramond, and R. Slansky, in *Supergravity*, eds. P. van Nieuwenhuizen and D. Freedman, (North Holland)(1979).
16. In the case where a ^{71}Ga rate of $\gtrsim 100$ SNU is measured, a measurement of the ^8B solar neutrino spectrum (see Rosen and Gelb ref. 6) or the flavor independent solar neutrino spectrum (see S. Weinberg, *XXIII International Symposium on High Energy Physics*, Berkeley, July 1986) would allow us to distinguish between changes in the solar model and resonant neutrino oscillations.

Table I

Neutrino Sources and Capture Rates for Two Solar Models

Process	E_{ν}^{max} (MeV)	Chlorine (SNU)		Gallium (SNU)	
		Model A	Model B	Model A	Model B
^8B	14.06	4.3	5.75	16.0	18.0
^7Be	0.861(90%) + 0.383(10%)	1.0	1.1	27	34
p-p	0.420	0	0	70	70
pep	1.44	0.23	0.20	2.5	3.0
^{13}N	1.199	0.08	0.10	2.6	4.0
^{15}O	1.732	0.26	0.35	3.5	6.0
Total		5.9	7.5	122	135

Figure Captions

Figure 1: Fits to the solar model of Bahcall: (a) is $\rho Y_e = m_N N_e$ and (b) is $(r/R_{\text{sun}})^2$ times the fractional neutrino volume emissivity for the indicated process, both as functions of fractional solar radius.

Figure 2: Neutrino capture cross sections as a function of energy for both ^{37}Cl and ^{71}Ga .

Figure 3: Iso-SNU contours for the ^{37}Cl experiment for the solar models listed in Table I. The contours are labeled with their the corresponding SNU values.

Figure 4: Iso-SNU contours for a ^{71}Ga detector for the solar models listed in Table I. We show 3σ deviations from the Davis ^{37}Cl experimental result by the dotted contours. The solid curves are labeled with their appropriate ^{71}Ga SNU values.

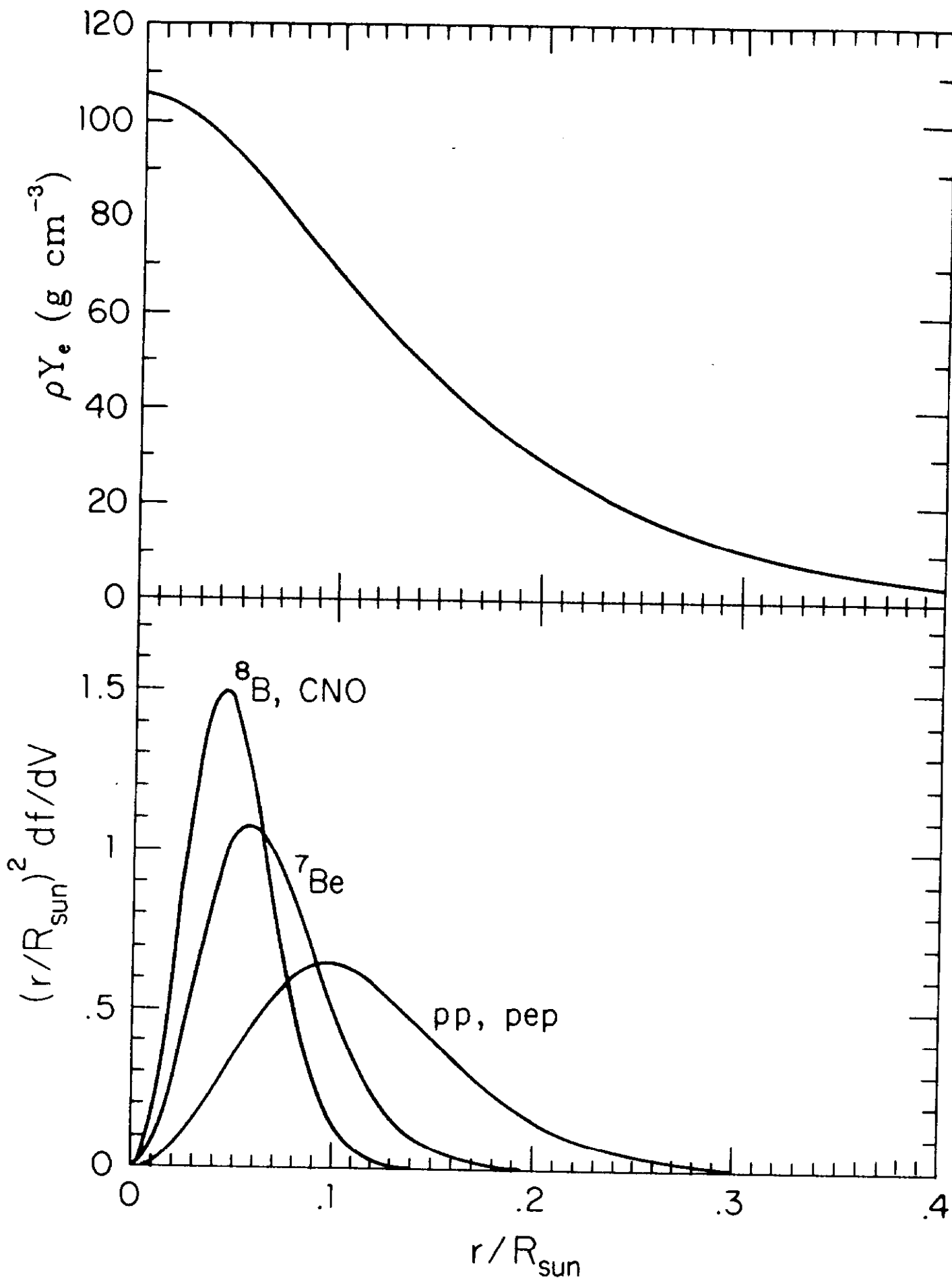


Fig. 1

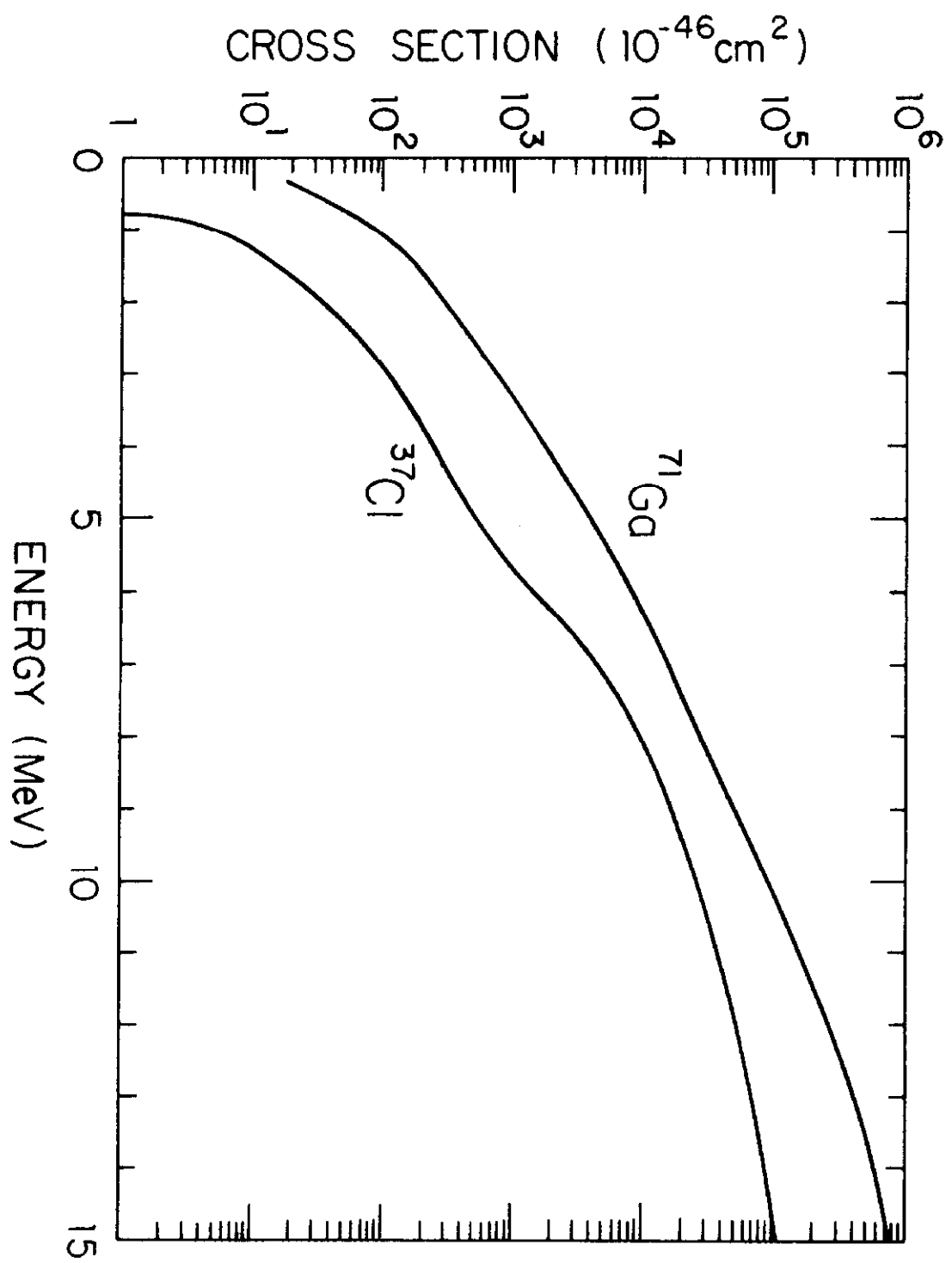


Fig. 2

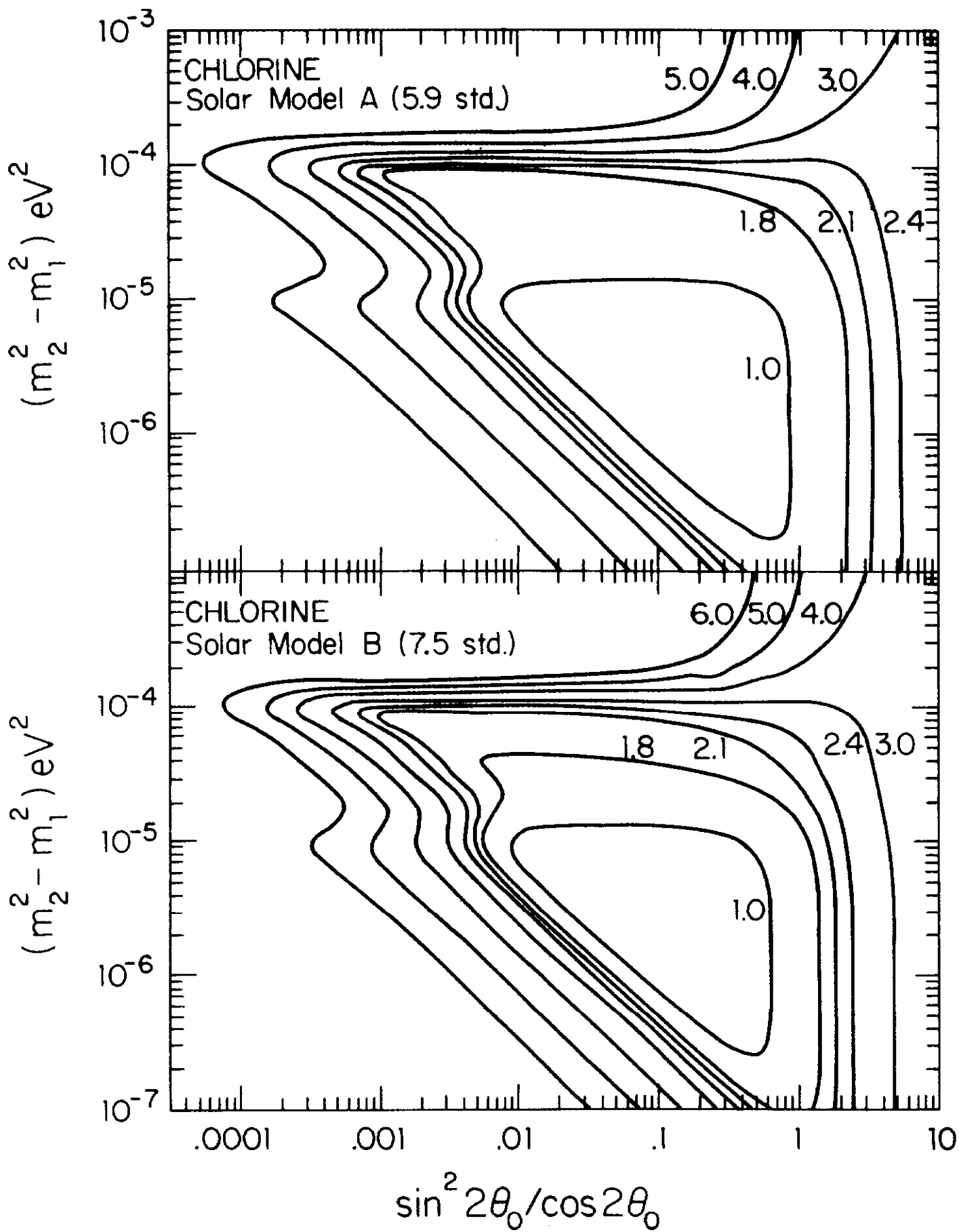


Fig. 3

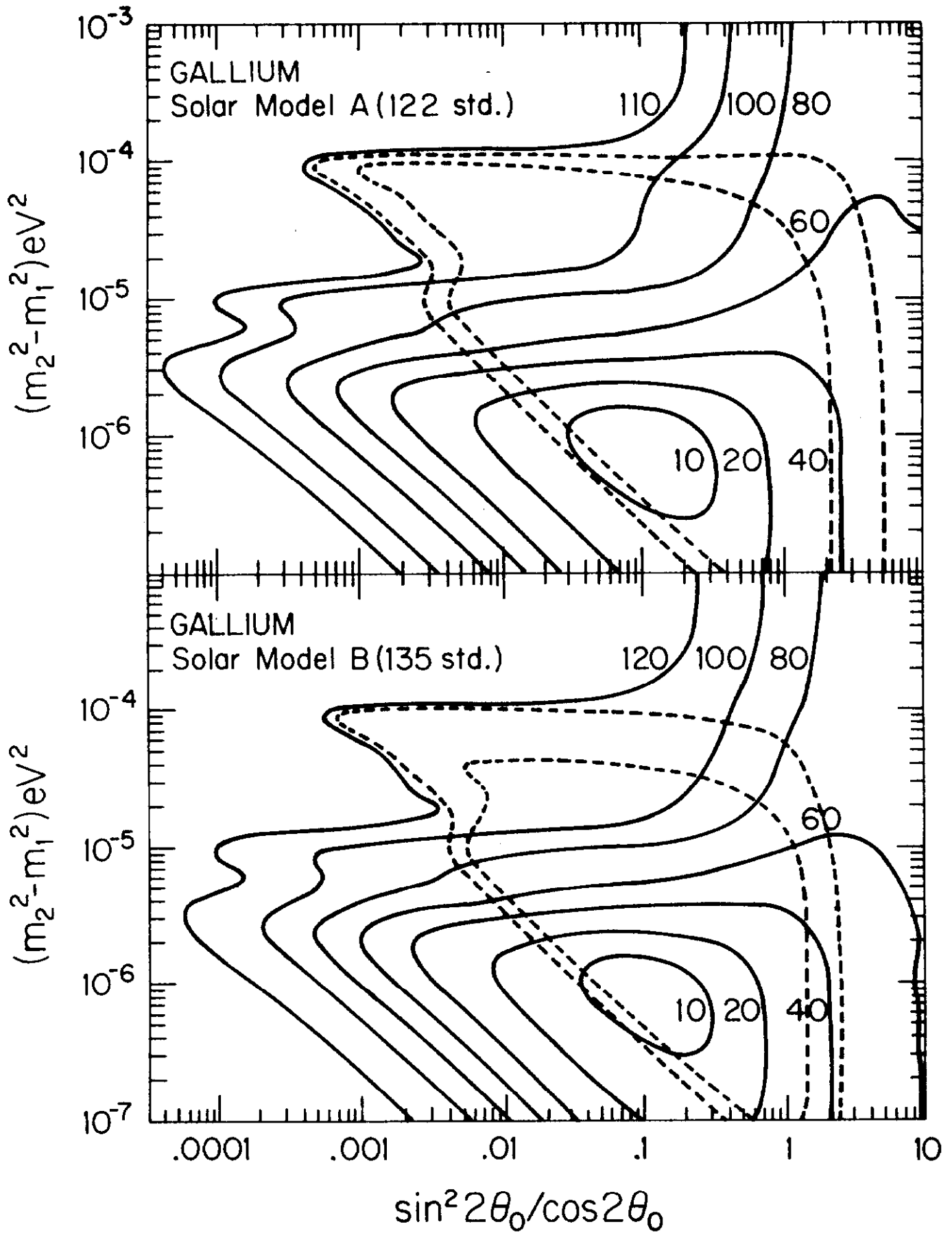


Fig. 4